International Journal of Research in Engineering and Science (IJRES)
ISSN (Online): 2320-9364, ISSN (Print): 2320-9356
www.ijres.org Volume 14 Issue 4 ǁ April 2026 ǁ PP. 86-97

Computer-Aided Design of Novel TRPC5 Inhibitors

Zheng Chang[1], Li Zhang[1, *]
[1]*School of Chemical Engineering, Sichuan University of Science & Engineering, Zigong 643000, China*
First author: (Kang Wang)
**Correspondence author: (Li Zhang)*

Abstract

Transient receptor potential channel TRPC5 is a critical calcium-permeable ion channel that plays an important role in the pathogenesis of neurological disorders, anxiety, and depression, making it a valuable target for drug discovery. In this study, computer-aided drug design (CADD) methods were employed to identify novel TRPC5 inhibitors.

First, a three-dimensional structural model of the TRPC5 protein was obtained from the PDB database. Binding site prediction was then used to locate the putative drug-binding pockets. Using SML-13, a previously identified TRPC5 inhibitor from our research group, as the lead compound, we performed precise molecular docking of SML-13 with the crystal structure of TRPC5 (PDB: 7D4Q) using Schrödinger software. Analysis of the binding mode rThe evealed that the central pyrimidine ring serves as the key scaffold for maintaining activity, forming stable π-π stacking interactions with residues such as TRP577 and PHE576 in the binding pocket, thereby providing an essential anchoring core for the molecule. The Inspirator module of SeeSAR was then employed for pharmacophore-based replacement to optimize the structure, leading to the identification of compounds with potential inhibitory activity. Through further structural modifications and structure–activity relationship (SAR) studies, a series of novel TRPC5 inhibitors were designed, and their stability and binding modes were analyzed via molecular dynamics simulations. In vitro assays demonstrated that the designed compounds exhibited good and stable inhibitory activity against TRPC5. Subsequent cytotoxicity and pharmacokinetic studies indicated that the optimized compounds had low toxicity and favorable bioavailability.

This work successfully established a computer-aided design strategy for TRPC5 inhibitors, which is of great significance for the development of new drugs for related neuropsychiatric disorders and also provides novel ideas and methods for ion channel-targeted drug discovery.

Key words: *TRPC5; computer-aided drug design; molecular docking; inhibitors; pharmacophore screening*

Date of Submission: 09-04-2026 Date of Acceptance: 22-04-2026

I. Introduction

1.1 TRPC5

The TRPC5 ion channel is widely distributed in tissues and organs including the central nervous system, cardiovascular system, and urinary system, and its aberrant activation is closely associated with the onset and progression of various diseases[1]. Although ion channel-targeted drugs account for approximately 9% of the global pharmaceutical market (with a market size of about 281 billion USD), highly selective inhibitors against TRPC5 remain scarce[2]. Existing modulators generally suffer from poor selectivity and significant side effects, which severely limit their clinical application[3]. TRPC5 plays a critical role in several major diseases: in the central nervous system, its overactivation leads to neuronal death, synaptic dysfunction, and cognitive decline. The number of Alzheimer's disease patients worldwide is projected to increase from approximately 47 million in 2024 to 131 million by 2025, while the number of Parkinson's disease patients rose from 8.9 million in 2019 to over 10 million in 2023. In the kidney, aberrant expression of TRPC5 is associated with chronic kidney disease, which affects more than 850 million people globally[4]. Furthermore, TRPC5 dysfunction is also linked to obesity, maladaptive behaviour, and postpartum depression[5].

TRPC5 belongs to the canonical subfamily of transient receptor potential (TRP) channels and is the fifth member of the TRPC family[6]. Its structure exhibits typical TRP channel features: a tetramer assembled from six transmembrane helices (S1–S6), an N-terminal ankyrin repeat domain, and a C-terminal TRP domain essential for channel assembly and function[7,8]. Unlike other TRPC members, TRPC5 and TRPC4 are insensitive to diacylglycerol (DAG). Instead, they are activated via the Gq/11-PLC pathway: hydrolysis of PIP_2 generates IP_3, which activates IP_3 receptors and triggers Ca^{2+} release from intracellular stores, elevating cytosolic Ca^{2+} concentration and thereby opening the channel. In addition, extracellular di- or trivalent cations (e.g., La^{3+}, Gd^{3+}) can enhance channel activity by coordinating with Glu543 and Glu595[9] (**Figure 1**). Recent studies have also shown that the adaptor protein NHERF interacts with the C-terminus of TRPC5 via its PDZ domain, modulating the channel's sensitivity to DAG.[10]

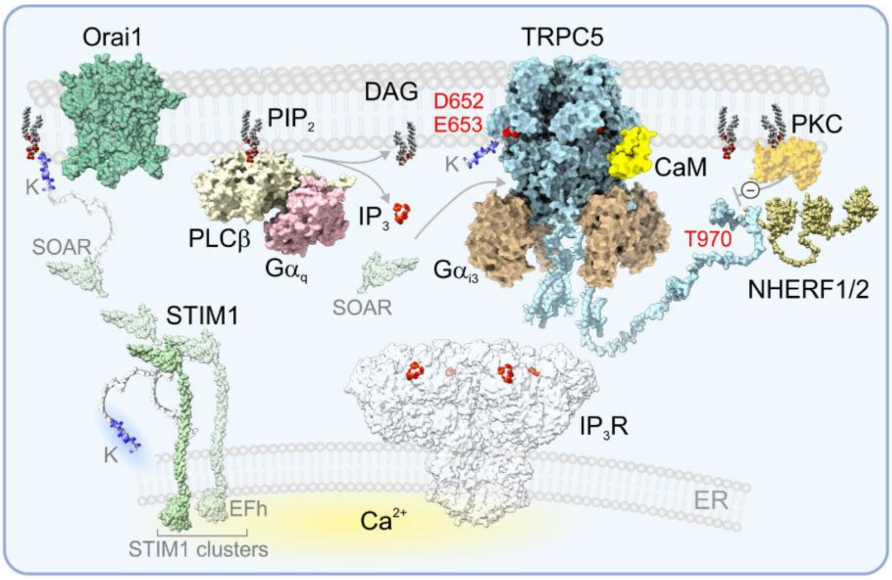

Figure 1 Schematic diagram of the primary interactions between the TRPC5 channel and signaling proteins in a cellular context

In structural biology, a high-resolution cryo-EM structure of TRPC5 was resolved in 2019, and by 2025 the PDB database had deposited 25 distinct conformations (22 human, 3 murine)[11]. The TRPC5 subunit contains a voltage-sensor-like domain formed by S1–S4, a pore domain between S5 and S6, and a cytoplasmic region with four ankyrin repeats and a helix-loop-helix domain at the N-terminus, as well as a connecting helix and a coiled-coil domain together with an intrinsically disordered region at the C-terminus, the latter being involved in channel localisation and protein-protein interactions[12]. From a drug design perspective, multiple potential drug-binding sites exist on the TRPC5 channel (transmembrane, intracellular, and extracellular). Among these, the binding sites of CMZ (**Figure 2**) and HC-070 (**Figure 3**) have been shown to be important for inhibitor development[13].

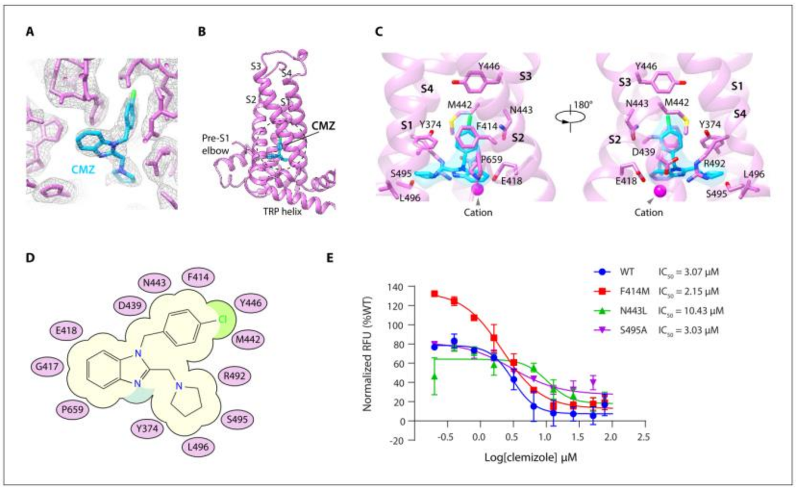

Figure 2 Binding of the inhibitor CMZ (IC_{50} = 3.03 μM) to TRPC5

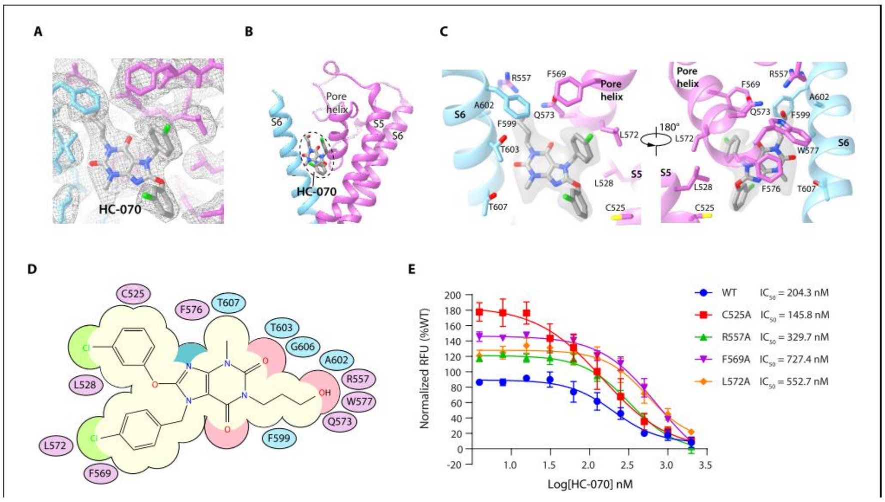

Figure 3 Binding of the inhibitor HC-070 ($IC_{50} = 3.03\ \mu M$) to TRPC5

Regarding function and pathology, under normal physiological conditions TRPC5 maintains neuronal excitability, synaptic plasticity, and dendritic spine stability; its dysfunction impairs learning and memory[14,15]. In Alzheimer's disease, deposition of β-amyloid can activate TRPC5 and exacerbate neuronal injury[16]. Overactivation, however, leads to calcium overload and activation of signalling pathways such as calcineurin, triggering cytoskeletal remodelling, foot process effacement, and podocyte death, ultimately resulting in proteinuria and chronic renal failure[17]. Moreover, TRPC5 is overexpressed in various malignant tumours including prostate, breast, lung, and gastric cancers, promoting tumour cell proliferation, invasion, and metastasis[18]. TRPC5 inhibitors may therefore directly suppress malignant progression and, in combination with conventional chemotherapy, enhance efficacy while reducing toxicity.

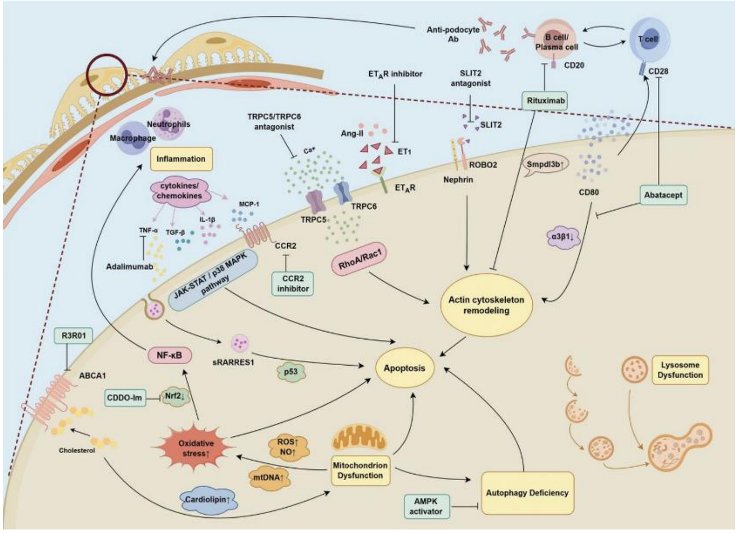

Figure 4 Mechanisms of Podocyte Injury and Associated Pharmacological Targets

In summary, TRPC5 has emerged as a promising drug target for kidney diseases, neurological disorders, and cancer. The development of potent and selective TRPC5 inhibitors holds significant value for basic research and clinical translation.

1.2 Current Landscape of TRPC5 Inhibitors

In recent years, TRPC5 has emerged as a promising therapeutic target for kidney diseases, neurological disorders, and tumor multidrug resistance. Structural analyses of TRPC5 in complex with various inhibitors and activators have been reported. Based on their chemical scaffolds, known TRPC5 inhibitors fall into five categories: benzimidazoles[19], quinolines[20], flavonols[21], pyridazinones[22], and xanthines[23] (**Figure 5**).

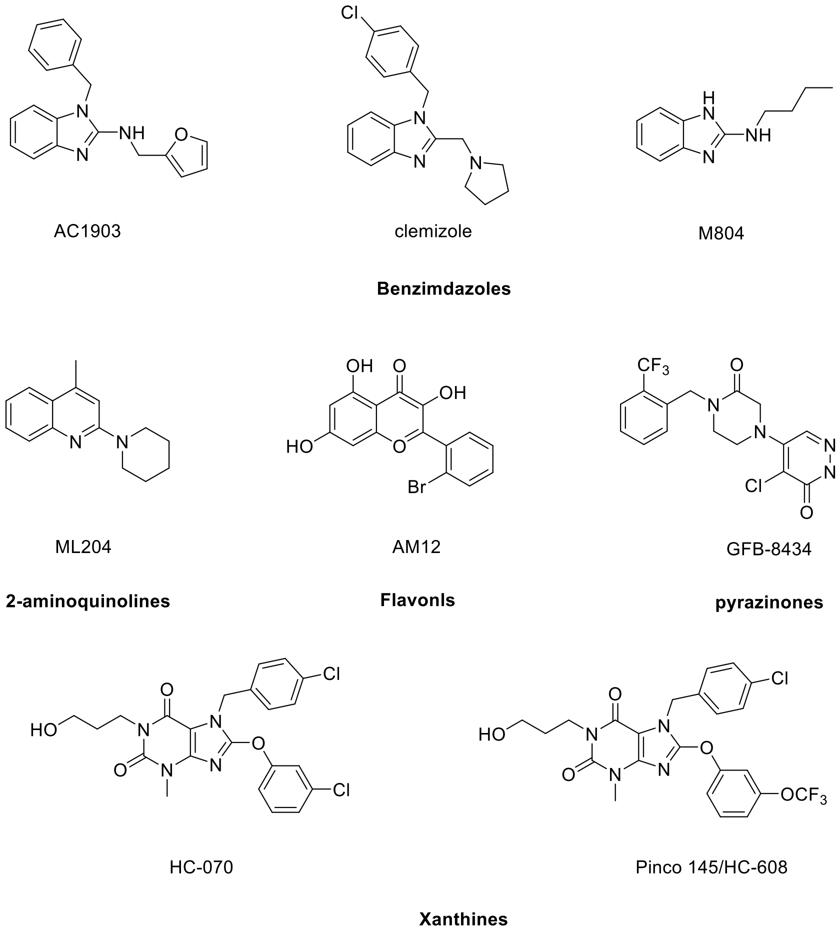

Figure 5 Recently reported TRPC5 inhibitors

Among these, ML204 was the first potent and selective small-molecule inhibitor of TRPC4/C5. It was identified through high-throughput fluorescence calcium imaging screening of over 300,000 compounds using a HEK293 cell line co-expressing mouse TRPC4β and the μ-opioid receptor. ML204 exhibits an IC_{50} of approximately 0.96 μmol/L for TRPC4β. Multiple validation experiments confirmed that it directly acts on the channel itself, with no appreciable inhibition of TRPC6, other TRP subfamily members, or voltage-gated ion channels; at 10 μmol/L it displays excellent selectivity. This work established an important methodological reference for the screening and validation of ion channel inhibitors.

Building on this foundation, Yiming Zhou and colleagues aimed to develop more specific TRPC5 inhibitors. Through systematic structural optimization and screening of more than 50 ML204 derivatives, followed by electrophysiological assessment using patch-clamp techniques, they identified AC1903 as a highly selective TRPC5 inhibitor. AC1903 has an IC_{50} of approximately 14.7 μmol/L for TRPC5 and does not significantly inhibit TRPC4 or TRPC6. In two animal models of proteinuric kidney disease, AC1903 markedly reduced proteinuria progression, decreased podocyte pseudocyst formation, and rescued podocyte loss, without affecting blood pressure or causing overt toxicity. Its mechanism involves blocking reactive oxygen species generation and cell death mediated by the Rac1–TRPC5 signaling pathway in podocytes.

Another noteworthy class is the xanthine derivative HC-070. Its precursor, HC-608, was identified through high-throughput screening but exhibited low brain uptake. Through systematic structure–activity relationship studies, the research team optimized HC-608 to yield HC-070, which has an IC_{50} as low as 9.3 nmol/L for TRPC5 and shows >400-fold selectivity over other channels. Although HC-070 demonstrated excellent preclinical profiles, its highest stage of development reached only Phase I clinical trials (for anxiety and depression), and it has not advanced to later-stage clinical testing.

Natural products have also yielded TRPC5 inhibitors. For example, from the flavonol class, AM12 was derived from galangin isolated from Zingiberaceae plants. Structure–activity relationship studies revealed that the hydroxyl substitution pattern on the flavonoid core and ortho-substitution on the phenyl ring are critical for activity. The designed compound AM12 (IC_{50} = 0.28 μmol/L) retains the flavonoid scaffold while incorporating an ortho-bromine atom. It inhibits lanthanide-induced Ca^{2+} influx in differentiated 3T3-L1 cells, but it also inhibits TRPC4.

To date, no TRPC5 inhibitor has been approved for clinical use, and most candidates remain at the preclinical stage. Several key challenges hinder clinical translation. Selectivity optimization remains a central difficulty: ML204 exhibits varying degrees of inhibition of TRPC4 and TRPC6, and although AC1903 substantially improves selectivity, systematic validation is still required to rule out off-target effects within the same family. Most studies are limited to preclinical animal models, and clinical data are lacking; the safety, pharmacokinetic properties, and long-term tolerability of candidate drugs in humans remain undefined. Natural products such as AM12 show potent in vitro activity, but their in vivo efficacy and metabolic stability are poorly characterized. Furthermore, compound optimization still relies heavily on traditional screening and modification strategies with low efficiency. Leveraging structural biology and artificial intelligence to accelerate the discovery of novel scaffolds and improve optimization efficiency represents a key direction for future breakthroughs.

1.2 Computer-Aided Drug Design

Computer-aided drug design (CADD) encompasses a set of computational techniques for discovering, developing, and analyzing drug molecules and bioactive compounds with similar physicochemical and biochemical properties[24]. It includes homology modeling, molecular docking, virtual screening, quantitative structure–activity relationship (QSAR) analysis, and 3D pharmacophore mapping. CADD is now widely used in drug discovery, and numerous approved drugs have benefited from computational support (**Figure 6**).

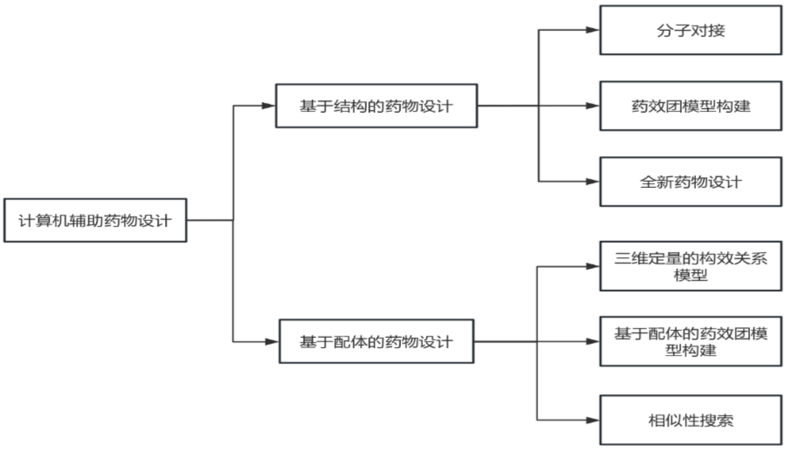

Figure 6 Classification of computer-aided drug design

CADD is broadly divided into structure-based drug design (SBDD) and ligand-based drug design (LBDD)[25]. SBDD relies on the three-dimensional structure of the target protein, obtained from X-ray crystallography, NMR spectroscopy, or cryo-electron microscopy. It employs techniques such as molecular docking to investigate receptor–ligand interactions, energetic complementarity, and spatial fit, thereby identifying active compounds or predicting potential molecular structures through de novo design. LBDD, on the other hand, is used when the target structure is unknown. It analyzes the two- or three-dimensional structures, structure–activity relationships, and pharmacophore features of known active ligands to extract key characteristics essential for biological activity[26]. Lead compounds are then discovered using methods such as similarity searching, substructure searching, pharmacophore screening, and 3D-QSAR.

A classic success story of CADD is the development of captopril[27] (**Figure 7**), the first oral angiotensin-converting enzyme (ACE) inhibitor. Researchers constructed a model of the ACE active site based on the structure of the BPF peptide from the venom of the Brazilian pit viper (Bothrops jararaca), leading to the design of a molecule with stable antihypertensive effects and long-term benefits.

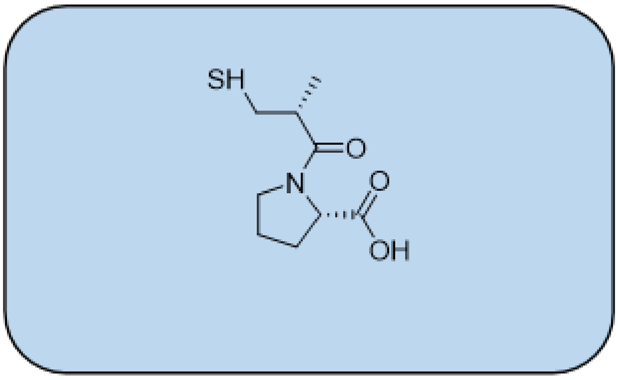

Figure 7 Structure of Captopril

Molecular docking is a core CADD technique used to predict the optimal binding mode and affinity of a small-molecule ligand to a target protein[28]. The underlying principles draw on the lock-and-key and induced-fit models, using computer simulations to assess geometric and energetic complementarity within the active site. Docking strategies fall into three categories[29]: rigid docking (no conformational change in the system, suitable for large complexes such as protein–protein or protein–nucleic acid interactions), semi-flexible docking (the ligand conformation is allowed to rotate within limits, commonly used for compound–protein docking), and fully flexible docking (all conformations can change freely, providing high accuracy but at greater computational cost)(**Figure 8**).

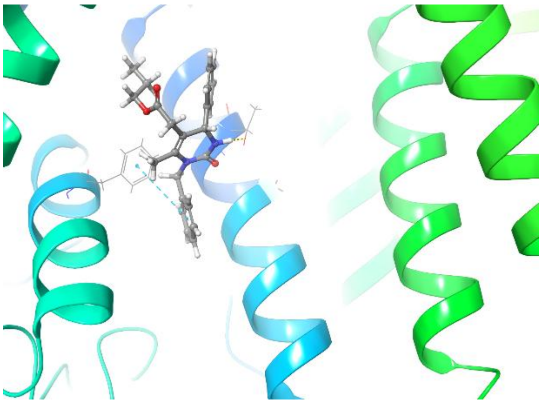

Figure 8 Binding mode of the compound to the protein

Pharmacophore replacement is a highly effective and mature molecular optimization strategy in CADD. It replaces key structural fragments (functional groups, ring systems, or side chains) in a molecule to explore new chemical space, improve physicochemical properties, and retain or enhance binding activity. Major strategies include[30]:

(1) Scaffold hopping: replacing the core scaffold with different types of cores (e.g., heterocycles, spiro rings) while preserving the spatial orientation of key pharmacophore features.

(2) Fragmen-based replacement: analyzing "empty regions" in the pharmacophore model and searching databases for new fragments that maintain pharmacophore overlap but offer smaller molecular weight or higher ligand efficiency.

(3) Receptor-guided replacement: when the target crystal structure is known, analyzing the properties of residues in the binding pocket to replace ligand side chains with groups that introduce new interactions such as salt bridges or π-π stacking.

(4) Shape-matched replacement: emphasizing the overall molecular shape and electrostatic/volumetric complementarity with the pharmacophore space, replacing a region with a group that occupies the same volume but has a different chemical structure to maintain or enhance selectivity.

In practice, medicinal chemists often combine multiple strategies. For example, structure-based pharmacophore mapping and molecular docking may first identify key residue interactions, followed by fragment shape matching and functional group replacement to further optimize the compound. The integrated use of these computational techniques has greatly improved the efficiency and success rate of drug discovery.

II. Result

2.1 Lead compound analysis

SML-13 is a bioactive small molecule previously identified by our research group through a pharmacophore model constructed from the cryo-EM structure of the TRPC5–HC-070 complex (PDB: 7D4Q), followed by multi-step virtual screening. In vitro calcium flux assays demonstrated that SML-13 inhibits TRPC5 with an activity (IC_{50} = 10.3 μM) comparable to that of the positive control AC1903. Compared with HC-070, SML-13 features a simpler structure: a pyrimidine core that extends into two phenyl rings and an ester-containing tail. The molecule possesses moderate backbone rigidity and a straightforward synthetic route. Moreover, it retains high structural modifiability in distinct regions, facilitating strategies such as halogen introduction, aliphatic chain extension, or incorporation of hydrogen-bond donors/acceptors to further enhance binding affinity to TRPC5 and improve subtype selectivity. On this basis, SML-13 was selected as the lead molecule for systematic structure optimization and structure–activity relationship studies in the present work.

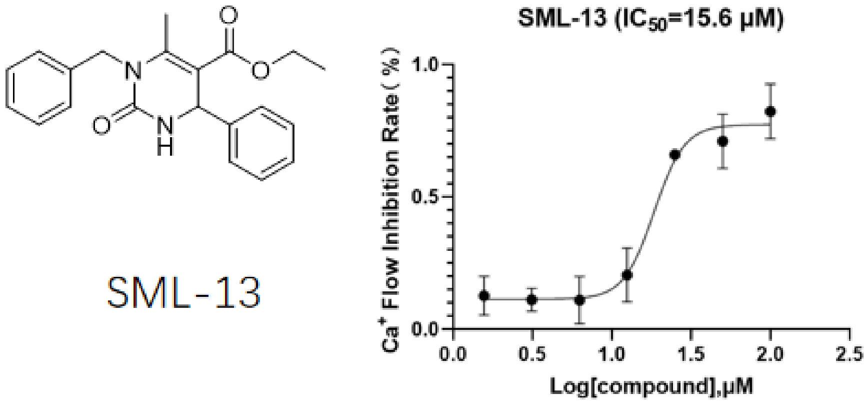

Figure 9 Structure and IC_{50} Value of SML-13

To elucidate the binding mode of SML-13 with TRPC5, we performed precise molecular docking using the Schrödinger suite (Glide module, extra precision) against the crystal structure of TRPC5 (PDB: 7D4Q). The docking results showed that SML-13 fits snugly into a hydrophobic binding cavity lined by 19 key residues, including TRP577, PHE576, PHE599, GLN573, and ARG557. The central pyrimidine ring engages in a stable π-π stacking interaction with TRP577, while the carbonyl oxygen on the ring forms an additional hydrogen bond with the indole NH of TRP577. Together, these interactions constitute the core anchoring framework that underpins the inhibitory activity of SML-13. Further analysis of the hydrophobic/hydrophilic properties of the binding cavity using Discovery Studio software indicated that the entire SML-13 molecule resides in a large hydrophobic pocket, and the regions surrounding the pyrimidine-linked phenyl ring and the ester tail offer considerable room for modification. This provides a clear structural rationale for subsequent region-based optimization (**Figure 10**).

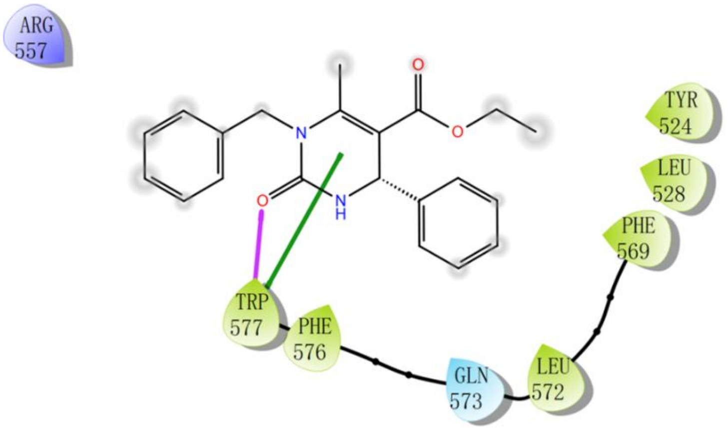

Figure 10 2D interaction mode of SML-13

2.2 Design of SML-13 Derivatives

Based on the interaction analysis of the lead compound SML-13, we divided SML-13 into three modifiable regions: Region I (the left-side phenyl ring and heterocyclic replacement region), Region II (the aliphatic chain region connecting the ester group), and Region III (the right-side phenyl ring and tail region).

These three regions reside in distinct microenvironments within the binding cavity. Region I lies in a relatively narrow hydrophobic groove and is sensitive to the bulk of substituents. Region II consists of an aliphatic chain that extends deep into the cavity; the degree of complementarity between its length and the cavity may significantly influence binding stability. Region III is a flexible linkage, where adjustments to the connection mode and introduction of polar groups can be explored to establish new interactions. In this study, we focused on these three regions and employed a pharmacophore replacement strategy (using the Inspirator module of SeeSAR). While retaining the central pyrimidine scaffold and its key interaction with TRP577, we performed systematic scaffold hopping, chain length adjustment, and introduction of polar groups on the substituents in each region, aiming to obtain novel TRPC5 inhibitors with higher binding affinity and improved selectivity. The above molecular docking and cavity analysis provide clear direction for subsequent structure optimization and a reliable structural basis for pharmacophore replacement-based drug design (**Figure 11**).

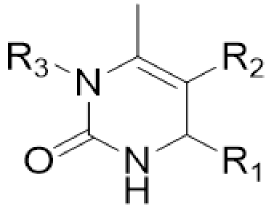

Figure 11 Three modifiable regions of SML-13

2.3 Drug design workflow

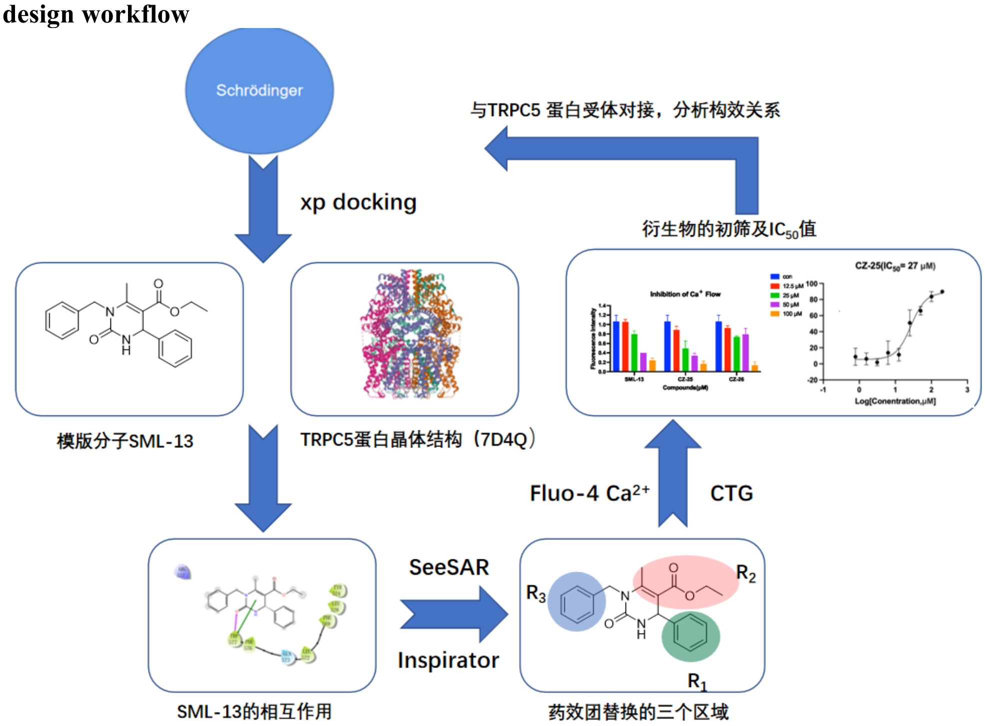

2.4 Identification of Hit Compounds

Based on the above strategy, we performed modifications on each of the three regions using computer-aided drug design. Through visual inspection of the docking poses, we identified compounds with potential activity, which were subsequently synthesized and subjected to preliminary activity screening (**Figure 12**). exhibited higher inhibitory activity than the lead compound across the concentration range of 25 μM to 100 μM.

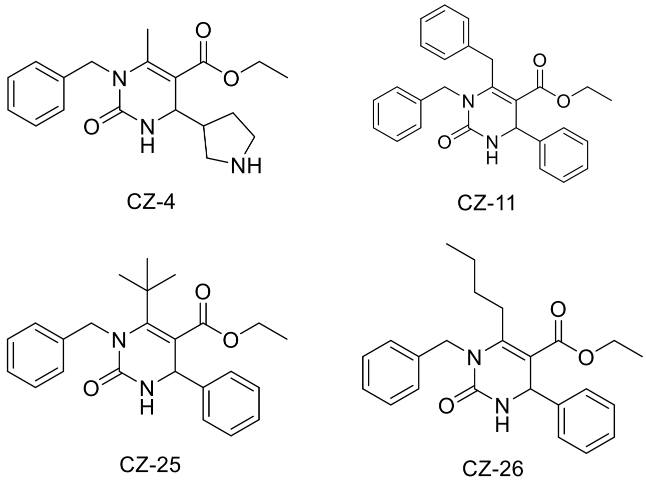

Figure 12 Compound structures of candidate compounds CZ-4、CZ-11、CZ-25、CZ-26

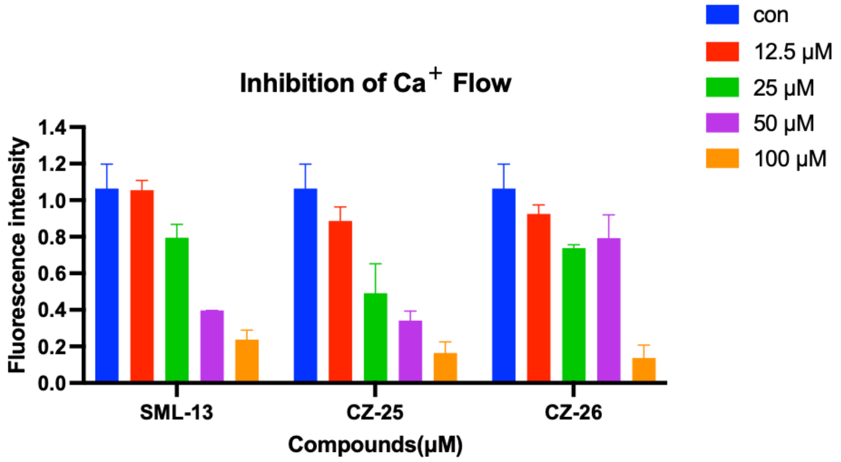

Figure 13 Primary screening inhibitory activity of CZ-25 and CZ-26

Table 1 Primary screening inhibitory activity of CZ-4、CZ-11、CZ-25、CZ-26

Compound	R	Fluorescence intensity			IC$_{50}$(μM)
		25μM	50μM	100μM	
SML-13	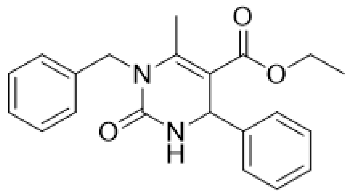	0.80	0.40	0.24	15.6
CZ-4	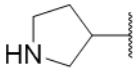	0.36	0.40	0.38	/
CZ-11	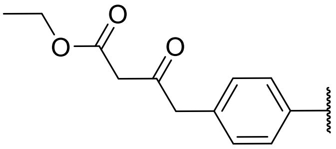	1.0	0.8	0.37	/
CZ-25	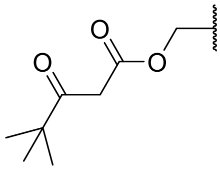	0.49	0.34	0.16	/

CZ-26	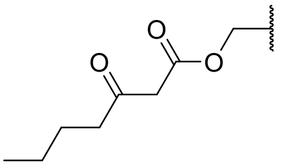	0.74	0.79	0.14	/

III. Discussion

The modification results for Region I indicate that the binding cavity in this region is relatively narrow and highly sensitive to the volume of substituents. Although CZ-4 formed a hydrogen bond with the key residue THR603 via the amino group on its five-membered heterocycle and showed moderate activity at 25 μM, its inhibitory activity was lower than that of the positive compound SML-13 at concentrations ranging from 50 μM to 100 μM. Overall, most derivatives exhibited poor inhibitory activity, confirming the limited scope for modification in this region.

Modifications in Region II yielded a notable breakthrough in enhancing the inhibitory activity of the compounds. By adjusting the length of the aliphatic chain, we found that the degree of complementarity between the chain length and the binding cavity significantly influences inhibitory activity. CZ-25 exhibited superior inhibitory activity to SML-13 across the concentration range of 25–100 μM. Molecular docking results indicated that an appropriately extended aliphatic chain penetrates deeper into the hydrophobic cavity, enhancing hydrophobic interactions. Meanwhile, the amino group on the pyrimidine ring or the phenyl ring formed hydrogen bonds and π-π stacking with key residues, synergistically improving binding affinity. In contrast, excessive chain length (CZ-26) led to a decrease in activity, further confirming that cavity complementarity is a key determinant of activity.

The modifications in Region III focused on balancing flexibility and rigidity in the linking moiety. Early designs, such as replacing the phenyl ring with a three-membered ring, resulted in a complete loss of activity due to excessive rigidity and insufficient volume. Although introducing a cyano group linked via a flexible methylene spacer (CZ-20) led to some improvement, the activity remained lower than that of the lead compound SML-13. Therefore, the original phenyl ring attached through a methylene linker was retained in this region.

IV. Methods

4.1 Protein preparation

Prior to molecular docking, the protein receptor and small-molecule ligands were first preprocessed. The crystal structure of the TRPC5 protein (PDB ID: 7D4Q) was downloaded from the PDB database and imported into the Protein Preparation Wizard module of Schrödinger. The following steps were performed sequentially: addition of missing hydrogen atoms, calculation of the protonation states of ionizable residues at physiological pH using the PROPKA algorithm, side-chain optimization (with particular attention to residues near the binding pocket), and removal of unnecessary water molecules and metal ions. Finally, the complex was subjected to restrained energy minimization using the OPLS3e force field to optimize the energy while preserving the overall backbone conformation. The docking grid was generated centered on the coordinates of the original ligand SML-13, with a box size of 10–20 Å to encompass the key binding residues.

4.2 Ligand preparation

The processing of the small-molecule ligand SML-13 was carried out using the LigPrep module. Its two-dimensional structure or SDF file was imported, and the Epik module was invoked to predict protonation states and ionization forms within a pH range of 7.0 ± 2.0. Energy minimization was performed using the OPLS3e force field, and possible stereoisomers and tautomers were automatically generated. Finally, a canonical three-dimensional structure file was output.

4.3 Protein docking

Molecular docking was performed using the Glide module with the extra precision (XP) mode. Given the limited number of ligands to be docked and the need for high-accuracy binding poses, the standard precision (SP) mode was bypassed. After docking, the Ligand Interaction module was used to visualize and analyze interactions between the ligand and the protein, including hydrogen bonds, π-π stacking, and hydrophobic contacts.

4.4 Pharmacophore replacement

Pharmacophore replacement was performed using the Inspirator module of SeeSAR. The structure of SML-13 was imported, and the replacement range (1.5–2.5 Å) was defined via the "Define New Constraints" function. Pharmacophoric constraints (e.g., aromatic rings, aliphatic chains) were then applied. Core replacement was carried out using the built-in structural database to screen for new fragments that satisfied the constraints, generating candidate compounds. Finally, visual inspection was performed to select molecules suitable for organic synthesis.

V. Conclusion

In this study, we implemented a computer-aided drug design (CADD) strategy to discover and optimize novel TRPC5 inhibitors, a class of compounds with potential therapeutic value for kidney diseases, neurological disorders, and other TRPC5-related pathologies. Using the crystal structure of TRPC5 (PDB: 7D4Q) and the lead compound SML-13 as a starting point, we performed structure-based molecular docking to identify the essential pharmacophore (the central pyrimidine ring) and divided the molecule into three modifiable regions. Guided by this analysis, we employed pharmacophore replacement using the SeeSAR Inspirator module to systematically explore chemical space, leading to the design and synthesis of a focused set of derivatives.

The biological evaluation of these derivatives, using fluorescence calcium flux assays and cell viability counter-screens, revealed clear structure–activity relationships that validated our CADD approach. For Region I, which resides in a narrow hydrophobic groove, the derivative CZ-4 (containing a five-membered heterocycle with an amino group) formed a hydrogen bond with THR603 and showed moderate activity at 25 μM. However, at higher concentrations (50–100 μM), its inhibitory activity fell below that of the lead compound SML-13, and most other derivatives in this region were inactive. These results confirm that Region I is highly sensitive to substituent volume and offers limited modification space, consistent with our docking-based prediction.

In contrast, modifications in Region II, which consists of an aliphatic chain extending into a hydrophobic cavity, yielded a notable breakthrough. Derivative CZ-25, bearing an optimized chain length, exhibited superior inhibitory activity to SML-13 across the full concentration range of 25–100 μM. Molecular docking suggested that the appropriately extended aliphatic chain achieves better cavity complementarity, enhancing hydrophobic contacts while allowing the pyrimidine ring and phenyl group to maintain key π-π stacking and hydrogen bonds with residues such as TRP577 and PHE576. Conversely, excessive chain elongation (as in CZ-26) led to a marked decrease in activity, further underscoring that precise chain-to-cavity matching is a critical determinant of potency.

For Region III, early attempts to replace the phenyl ring with more rigid or smaller groups resulted in loss of activity. Although the introduction of a flexible cyano-containing linker provided some improvement, the activity remained lower than that of SML-13. The data from CZ-11 (a derivative with a methylene-linked phenyl group) indicated only modest activity, reinforcing the importance of retaining an optimal balance between flexibility and steric bulk in this region.

Overall, the CADD-driven design and systematic evaluation of these derivatives demonstrate that pharmacophore-based replacement, guided by high-resolution docking and cavity analysis, is an effective strategy for optimizing TRPC5 inhibitors. The success with CZ-25—achieving consistently higher activity than the original lead—validates the importance of fine-tuning aliphatic chain length to match the hydrophobic pocket. At the same time, the limited success in Regions I and III highlights the challenges posed by sterically constrained or poorly defined binding sub-pockets, which require more sophisticated optimization strategies in the future.

In summary, this work provides a practical CADD framework for the rational design of TRPC5 inhibitors, delivering a promising optimized derivative (CZ-25) with improved potency and a clear structure–activity rationale. The findings also underscore the value of combining computational predictions with empirical validation. Future efforts should focus on further improving selectivity over closely related TRPC channels (e.g., TRPC4 and TRPC6) and evaluating the in vivo efficacy of CZ-25 and its analogs in animal models of TRPC5-mediated diseases.

References

[1] DATTILO M, PENINGTON N J, WILLIAMS K. Regulation of TRPC5 currents by intracellular ATP: Single channel studies[J]. Journal of Cellular Physiology, 2020.

[2] Ion channel drug discovery and modern medicine[J], 2019.

[3] ZHOU Y, CASTONGUAY P, SIDHOM E-H, et al. A small-molecule inhibitor of TRPC5 ion channels suppresses progressive kidney disease in animal models[J]. Science, 2017.

[4] BIKBOV B, PURCELL C A, LEVEY A S, et al. Global, regional, and national burden of chronic kidney disease, 1990-2017: a systematic analysis for the Global Burden of Disease Study 2017[J]. The Lancet, 2020.

[5] LI Y, CACCIOTTOLO T M, YIN N, et al. Loss of transient receptor potential channel 5 causes obesity and postpartum depression[J]. Cell, 2024.

[6] MONTELL C, BIRNBAUMER L, FLOCKERZI V, et al. A unified nomenclature for the superfamily of TRP cation channels[J]. Molecular Cell, 2002.

[7] LIMAN E R, INNAN H. Relaxed selective pressure on an essential component of pheromone transduction in primate evolution[J]. Proceedings of the National Academy of Sciences of the United States of America, 2003.

[8] VANNIER B, ZHU X, BROWN D, et al. The membrane topology of human transient receptor potential 3 as inferred from glycosylation-scanning mutagenesis and epitope immunocytochemistry[J]. Journal of Biological Chemistry, 1998.

[9] FURUICHI T, SHIOTA C, MIKOSHIBA K. Distribution of inositol 1,4,5-trisphosphate receptor mRNA in mouse tissues[J]. FEBS Letters, 1990.

[10] LEE-KWON W, WADE J B, ZHANG Z, et al. Expression of TRPC4 channel protein that interacts with NHERF-2 in rat descending vasa recta[J]. American Journal of Physiology-Cell Physiology, 2004.

[11] DUAN J, LI J, CHEN G-L, et al. Cryo-EM structure of TRPC5 at 2.8-Å resolution reveals unique and conserved structural elements essential for channel function[J]. Science Advances, 2019.

[12] PTAKOVA A, VLACHOVA V. Thermosensing ability of TRPC5: current knowledge and unsettled questions[J]. The Journal of Physiological Sciences, 2024.

[13] SONG K, WEI M, GUO W, et al. Structural basis for human TRPC5 channel inhibition by two distinct inhibitors[J]. eLife, 2021.

[14] PURAM S V, RICCIO A, KOIRALA S, et al. A TRPC5-regulated calcium signaling pathway controls dendrite patterning in the mammalian brain[J]. Genes & Development, 2011.

[15] AHMED S R, LIU E, YIP A, et al. Novel localizations of TRPC5 channels suggest novel and unexplored roles: A study in the chick embryo brain[J]. Developmental Neurobiology, 2021.

[16] REZZANI R, FAVERO G, GIANò M, et al. Transient Receptor Potential Channels in the Healthy and Diseased Blood-Brain Barrier[J]. Journal of Histochemistry & Cytochemistry, 2024.

[17] SCHALDECKER T, KIM S, TARABANIS C, et al. Inhibition of the TRPC5 ion channel protects the kidney filter[J]. The Journal of Clinical Investigation, 2013.

[18] CHEN Z, ZHU Y, DONG Y, et al. Overexpression of TrpC5 promotes tumor metastasis via the HIF-1α/Twist signaling pathway in colon cancer[J]. Clinical Science, 2017.

[19] SHARMA S, PABLO J L, TOLENTINO K T, et al. Further exploration of the benzimidazole scaffold as TRPC5 inhibitors: identification of 1-alkyl-2-(pyrrolidin-1-yl)-1H-benzo[d]imidazoles as potent and selective inhibitors[J]. ChemMedChem, 2022.

[20] MILLER M, SHI J, ZHU Y, et al. Identification of ML204, a novel potent antagonist that selectively modulates native TRPC4/C5 ion channels[J]. Journal of Biological Chemistry, 2011.

[21] NAYLOR J, MINARD A, GAUNT H J, et al. Natural and synthetic flavonoid modulation of TRPC5 channels[J]. British Journal of Pharmacology, 2016.

[22] YU M, LEDEBOER M W, DANIELS M, et al. Discovery of a Potent and Selective TRPC5 Inhibitor, Efficacious in a Focal Segmental Glomerulosclerosis Model[J]. ACS Medicinal Chemistry Letters, 2019.

[23] JUST S, CHENARD B L, CECI A, et al. Treatment with HC-070, a potent inhibitor of TRPC4 and TRPC5, leads to anxiolytic and antidepressant effects in mice[J]. PLOS ONE, 2018.

[24] JIA P, PEI J, WANG G, et al. The roles of computer-aided drug synthesis in drug development[J]. Green Synthesis and Catalysis, 2022.

[25] NIAZI S K, MARIAM Z. Computer-Aided Drug Design and Drug Discovery: A Prospective Analysis[J]. Pharmaceuticals, 2023.

[26] GUTIéRREZ-DE-TERáN H, SALLANDER J, SOTELO E. Review on Computer-Aided Drug Design (CADD) Technique in Drug Discovery Researches and Solvent-Free Synthesis of 3,4-Dihydropyrimidin-2-(1H)-Ones/Thiones Catalyzed by Camphor Sulfonic Acid[J]. Biointerface Research in Applied Chemistry, 2022.

[27] MAHESAR S A, LAKHO S A, HUSSAIN SHERAZI S T, et al. Recent Progress in the Analysis of Captopril Using Electrochemical Methods: A Review[J]. Current Analytical Chemistry, 2019.

[28] MENG X-Y, ZHANG H-X, MEZEI M, et al. Molecular docking: a powerful approach for structure-based drug discovery[J]. Current computer-aided drug design, 2011.

[29] SAHU D, RATHOR L S, DWIVEDI S D, et al. A Review on Molecular Docking As an Interpretative Tool for Molecular Targets in Disease Management[J]. ASSAY and Drug Development Technologies, 2024.

[30] TERHORST J P, JORGENSEN W L. E/Z Energetics for Molecular Modeling and Design[J]. Journal of Chemical Theory and Computation, 2010.